

Numerical Study on the Hydraulic Performance of Submerged Porous Breakwater under Solitary Wave Attack

K. Al-Banaa[†] and P. L.-F. Liu[‡]

[†]Coastal and Air Pollution Department
Environment and Urban Development Division
Kuwait Institute for Scientific Research
P.O. Box : 24885
13109 Safat, KUWAIT.
kbanaa@kisir.edu.kw

[‡]School of Civil and Environmental Engineering
Cornell University, Ithaca
NY 14853, USA
pll3@cornell.edu



ABSTRACT

AL-BANAA, K., and LIU, P., 2007. Numerical Study on the Hydraulic Performance of Submerged Porous Breakwater under Solitary Wave Attack. Journal of Coastal Research, SI 50 (Proceedings of the 9th International Coastal Symposium), 201 – 205. Gold Coast, Australia, ISSN 0749.0208

The hydraulic performance of horizontally slotted submerged porous breakwater under solitary wave attack is investigated with the use of a well-validated two-dimensional model based on solving the Reynolds-Averaged Navier-Stokes (RANS) equations. A set of numerical experiments with various porosity, P , values are performed to evaluate the hydraulic performance of submerged breakwater in terms of the wave reflection, transmission, and dissipation coefficients. A comparison between the different methods for calculating the coefficients is also presented. The effect of porosity, P , values on the wave characteristics for an engineering application are calculated and discussed. For the sets of numerical experiments, only the weakly nonlinear solitary waves $H/h=0.10$ are considered. The solitary waves can be considered good representations of tsunami, storm surge and nonlinear shallow water waves.

ADDITIONAL INDEX WORDS: *Solitary wave, reflection, transmission and dissipation coefficients, weakly nonlinear solitary waves, porosity, tsunami, storm surge*

INTRODUCTION

Over the past few decades studies of wave-structure interactions have been a topic of popular and deep interest. The issues that have arisen from previous studies are related to a number of engineering concerns such as structural stability, scour, reduction of transmitted wave energy inside marinas and harbours and the evaluation of the hydraulic performance of breakwaters. To address these concerns, it is important to understand the characteristics of wave transformation during wave-structure interaction and subsequently the impact of waves on coastal structures. In order to protect coastal zones from wave attacks, the need arises to build protective structures such as breakwaters (submerged or emerged) or sea walls. Therefore, it is quite a challenge in coastal engineering to sustain the coast as a natural ecosystem and yet at the same time be able to maintain the beach for public use.

The conventional hard structures such as sea walls and submerged and emerged breakwaters are often made of rubble mound structures. Such structures are often not environmentally-friendly. Submerged porous breakwaters often perform remarkably better in damping waves and thus reducing wave reflections thereby protecting harbours and marinas from waves. Moreover, the submerged porous breakwater is able to enhance water circulation and exchange of water between the open sea and sheltered areas.

A lot of analytical work has been conducted for solitary wave transformations over a shelf. The analytical work has also been validated by using experimental data by GORING (1979) and

LOSADA *et al.* (1987). SEABRA-SANTOS *et al.* (1987) to further investigate the wave transformation over a shelf and submerged obstacle experimentally. Furthermore, the wave characteristics of breaking solitary waves over submerged obstacles were studied experimentally and numerically by GRILLI *et al.* (1994). Recently, studies of detailed flow in a solitary wave interaction with submerged obstacles have been investigated by CHANG *et al.* (2001). AL-BANAA (2005) has studied the solitary wave interaction with a vertical thin barrier experimentally and numerically by using Particle Image Velocimetry (PIV) and RANS model respectively.

In the case of a submerged porous breakwater, most of the studies only considered periodic waves and linear wave theory without considering the energy loss due to flow separation. In this study, a two-dimensional RANS model, as described in LIN and LIU (1998a, b), will be employed to evaluate the hydraulic performance of a submerged porous breakwater under solitary wave attack. The model is capable of describing viscous and rotational effects as well as turbulence. By using the model, the effects of porosity p on wave characteristic will be studied. For the sets of numerical experiments only the weakly nonlinear solitary waves $H/h=0.10$ will be considered. Three different methods are used to evaluate wave reflection, transmission and the dissipation coefficients (K_r , K_t , and K_d). Method 1 uses the energy integral method which is based on integration of the energy flux as described by LIN (2004). Method 2 utilises the equal partition concept to evaluate potential energy PE by integrating the transformed numerical wave gauge free surface data at a fixed location from spatial to temporal domain. The simplest analysis involved was in method 3. It was based on a derivation from linear

wave theory. In this approach, the hydraulic performance can be estimated by using only the ratio of different wave heights of the numerical wave gauge measurements at different time steps. The calculated coefficients by different methods will be discussed and compared.

COMPUTATIONAL MODEL

The computational model used in this study, which solves the two-dimensional Reynolds-Averaged Navier-Stokes (RANS) equations with κ - ϵ turbulence closure model, is applied to simulate numerical experiments for a different range of parameters. The ensemble-averaged velocity $\langle u_i \rangle$ and ensemble-averaged pressure $\langle p \rangle$ of a turbulent flow are governed by well-known RANS equations and can be expressed as

$$\frac{\partial \langle u_i \rangle}{\partial x_i} = 0 \quad (1)$$

$$\frac{\partial \langle u_i \rangle}{\partial t} + \langle u_i \rangle \frac{\partial \langle u_i \rangle}{\partial x_j} = -\frac{1}{\rho} \frac{\partial \langle p \rangle}{\partial x_i} + g_i + \frac{1}{\rho} \frac{\partial \langle \tau_{ij} \rangle}{\partial x_i} - \frac{1}{\rho} \frac{\partial \langle u_i' u_j' \rangle}{\partial x_j} \quad (2)$$

where $i, j = 1, 2$ and $\langle \tau_{ij} \rangle$ is the viscous stress. The term

$\rho \langle u_i' u_j' \rangle$ denotes the Reynolds stress exerted on the flow due to

the turbulent fluctuations. Furthermore, u_i' denotes the i -th component of the turbulence velocity and $\langle \rangle$ is the ensemble average. In the model, the Reynolds stress in Eq. (2) is modelled by the nonlinear stress-strain relationship to allow anisotropic turbulence. The Reynolds stress is calculated by the nonlinear eddy viscosity model as described in LIN and LIU (1998a). In the turbulence model, information on the turbulent kinetic energy (TKE), κ , and its rate of dissipation, ϵ , are required. Therefore, balance equations for both κ and ϵ are also solved. The detailed expressions for the nonlinear Reynolds stress model and κ - ϵ equations are lengthy and can be found in numerous literature, e.g. (LIN and LIU, 1998a, b). The model solves the RANS equations by two-step projection methods using the finite-difference formulation, while the forward time difference method is used to discretise the time derivatives. The convection terms are discretised by the combination of central difference method and the upwind method. The central difference method is used to discretise the pressure gradient as well as the stress gradient. A similar algorithm is used to solve the transport equations for κ and ϵ . The Volume of Fluids (VOF) method is implemented to track the free surface location as described by HIRT and NICHOLS (1981).

Approximate boundary conditions were used in this model. Zero stress condition was always imposed on the free surface and zero normal gradient boundary conditions were also imposed on κ and ϵ , suggesting that there was no turbulent leakage between the air and water interface. The mean velocity field was assumed to obey the log law of the wall locally near the solid boundary. Therefore, the wall shear stress as well as the friction velocity can be calculated and thus the mean velocity gradient and the values of κ and ϵ near the wall can also be estimated.

Two-dimensional integral energy equation (method 1)

One of the advantages of the RANS model is that it provides the temporal and spatial distributions of the ensemble-averaged velocity and the pressure fields can be utilised to estimate total mechanical energy (kinetic plus potential energy) in a defined controlled volume CV that may enclose various types of structures. By integrating the energy equation derived from the governing equations for a turbulent flow (RANS equation) with some manipulations and applying the Gauss divergence theorem, the rate of total energy flux through a control surface CS and the rate of local energy dissipation within the control volume CV can be deduced. The rate of total energy flux is the summation of the pressure induced energy flux, convective energy flux and energy fluxes induced by molecular and turbulence stress, while the rate of local energy dissipation is caused by molecular and turbulence stresses. Finally, the rate of change of total energy within the control volume CV will be reduced to a balance equation between the net energy flux in and out of the control surface CS and the total energy dissipation inside the control volume CV.

For the case of two-dimensional flow as shown in Figure (1), the corresponding CS is considered in a four sided rectangular domain. The top and bottom sides are considered to have no energy fluxes through them. Thus, the effective CS reduces to the left and right boundaries only (CS₁ and CS₂). The energy fluxes induced by molecular and turbulence stress can be neglected, in most cases, if one can choose CS₁ and CS₂ far away from the structures inside the computational domain. Therefore, the total energy balance can be reduced to a function of wave energy flux induced dynamic pressure and convective flow motion in and out of the CS on both sides. The formulation of the two-dimensional integral energy equation can be applied to define wave characteristics to study the hydraulic performance of a submerged porous breakwater. The final form of the two-dimensional integral of the total energy equation after integration between t_1 and t_2 will be simplified to

$$\int_{t_1}^{t_2} E dx dz + \int_{t_1}^{t_2} dt \int D dx dz = \left[\int_{t_1}^{t_2} dt \int_{-h(CS_1)}^{\eta(CS_1)} \langle P_D \rangle \langle u \rangle dz + \int_{t_1}^{t_2} dt \int_{-h(CS_1)}^{\eta(CS_1)} \frac{\rho}{2} \langle u \rangle \langle u^2 + w^2 \rangle dz \right] - \left[\int_{t_1}^{t_2} dt \int_{-h(CS_2)}^{\eta(CS_2)} \langle P_D \rangle \langle u \rangle dz + \int_{t_1}^{t_2} dt \int_{-h(CS_2)}^{\eta(CS_2)} \frac{\rho}{2} \langle u \rangle \langle u^2 + w^2 \rangle dz \right] \quad (3)$$

In the analysis, the selection of t_1 and t_2 can be wisely picked such that the integral of the first term in Eq. (3) inside the CV can be equal between t_1 and t_2 and thus can be neglected in the case of a solitary wave. With the above assumption, Eq. (3) can be reduced to

$$ED = (EP_{CS_1} + EC_{CS_1}) - (EP_{CS_2} + EC_{CS_2}) \quad (4)$$

In Eq. (4), EP_{CS_1} represents the integration of the energy flux induced dynamic pressure through CS₁ between t_1 and t_2 . EC_{CS_1} represents the integration of the convective energy flux through CS₁ between t_1 and t_2 . EP_{CS_2} & EC_{CS_2} are similarly defined. The ED represents the total energy dissipated inside the CV between t_1 and t_2 . The second terms on the right hand side of

Eq. (4) correspond only to the transmitted wave since only the transmitted wave passes through CS₂. As a result, Eq. (4) can be rewritten as

$$ED = (EP_{CS_1} + EC_{CS_1}) - (E_{trans}) \tag{5}$$

The E_{trans} term can simply be evaluated by integrating the total energy flux from t_1 to t_2 at CS₂. However, separation between the total energy fluxes associated with the incident and reflected waves mandates a careful approach. Separation between the two signals can be achieved by placing CS₁ away (upstream) from the structure. An intermediate time t_m , as shown in figure (2a), is then introduced to estimate the total energy flux associated with incident wave E_{inc} by integrating the signal from t_1 to t_m and reflected wave E_{ref} from t_m to t_2 . Once the total energy fluxes of incident, reflected and transmitted are known, the calculation of the wave reflection, transmission and dissipation coefficients (K_r , K_t , and K_d) can be defined as follows

$$K_r = \sqrt{\frac{E_{ref}}{E_{inc}}} \quad K_t = \sqrt{\frac{E_{trans}}{E_{inc}}}$$

$$K_d = \sqrt{\frac{ED}{E_{inc}}} = \sqrt{1 - K_r^2 - K_t^2} \tag{6}$$

Eq. (6) will be used as method 1 to evaluate the hydraulic performance of the submerged porous breakwater.

Equal partition (method 2)

The potential energy PE is the result of displacing a mass of the free surface η from an equilibrium position against a gravitational force. Due to the lack of spatial and temporal resolved data, many researchers assume the equal partition concept to evaluate the hydraulic performance of structures. The PE can be obtained by integrating the transformed numerical wave gauge free surface data at a fixed location from spatial to temporal domains. The integration is obtained in the time domain by replacing dx by $c dt$. Therefore the PE equation can be defined as

$$PE = \frac{c\rho g}{2} \int_{t_1}^{t_2} \eta^2 dt \tag{7}$$

where c is the wave phase speed and can be defined as

$$c = \sqrt{gh \left[1 + \frac{H}{h} \right]} \tag{8}$$

In all numerical experiments, c was assumed to be constant. Eq. (7) was applied to estimate the PE associated with the incident, transmitted and reflected waves. The PE associated with the transmitted wave, PE_{trans} , can easily be evaluated by applying Eq. (7) at CS₂ from t_1 to t_2 . However, PE_{inc} and PE_{ref} can be evaluated at CS₁ away (upstream) from the structure as discussed in method 1 by introducing an intermediate time t_m to separate the incident and reflected waves. Once the PE of the incident, reflected and transmitted are known, the wave reflection, transmission and dissipation coefficients (K_r , K_t , and K_d) can be calculated as defined in Eq. (6).

Water elevation record (method 3)

Based on linear wave theory derivation, which considers the flow irrotational, the estimation of wave reflection, transmission and subsequently the dissipation coefficients (K_r , K_t , and K_d) depend solely on the wave height of the numerical wave gauges. The coefficients were determined based on the estimate of the energy associated with the numerical wave profiles. Therefore the coefficients in Eq. (6) can be rewritten as a function of wave heights

$$K_r = \frac{H_{ref}}{H_{inc}} \quad K_t = \frac{H_{trans}}{H_{inc}}$$

$$\text{and thus } K_d = \frac{H_d}{H_{inc}} = \sqrt{1 - K_r^2 - K_t^2} \tag{9}$$

Model verification

The model has already been rigorously tested and verified with a large pool of experimental data for different coastal problems. For example, in the surf zone, the model results were compared with experimental data for wave shoaling and breaking problems (LIN and LIU, 1998a,b; LIN *et al.*, 1999; LIU and CHENG, 2001). The results were compared in terms of ensemble averaged velocity and turbulence intensity. As for wave-structure interaction problems, the model results again showed good agreement with available experimental data. Wave interaction with porous structures was later modelled and tested by LIU *et al.* (1999). Moreover, in particular, for solitary wave interactions with structures, CHANG *et al.* (2001 & 2005) conducted experimental work by using Particle Image Velocimetry (PIV) to measure the velocity field in the vicinity of a submerged rectangular obstacle. The model results again showed an excellent agreement with the PIV measurements. The model later was used to estimate the solitary wave runup and force on a vertical thin barrier by LIU and AL-BANAA (2004). Using both experimental data and model results, formulae for maximum run-up height and maximum force exerted on the vertical barrier were derived. Finally, AL-BANAA (2005) compared the model results with PIV measured data for ensemble averaged velocities behind a vertical barrier to investigate solitary wave interactions with a thin vertical barrier. The agreements were in general good.

Overall, all studies using the present RANS model show good agreement between experimental data and model results for different types of coastal problems.

NUMERICAL RESULTS AND DISCUSSION

A series of numerical experiments have been performed for solitary wave propagating over a submerged porous breakwater. We denote h as the water depth and it is kept constant throughout the tests at 2.4 m. H is the amplitude of the incident solitary wave

(Figure 1). The breakwater porosity can be defined as $P = \frac{s}{e}$, with

a gap spacing, s and distance, e , between two adjacent element axes. This distance was varied ($P = 0, 0.10, 0.20$ and 0.50) to evaluate the hydraulic performance of the breakwater. In the numerical computations, the free-surface displacement η and the velocity components of a solitary wave are given as the inflow boundary conditions at $x=0$. They can be expressed as presented by LEE *et al.* (1982).

The computational domain is $0 < x < 60$ m and $0 < z < 4$ m, and the edge of the breakwater is located at $x=40$ m with thickness $d=0.18$ m. Different grid sizes have been tested to ensure that solutions being presented herein are not grid dependent. The typical grid sizes used are $\Delta z=0.02$ m and $\Delta x=0.06$ m. The time

step size is determined dynamically so that the numerical stability condition is satisfied.

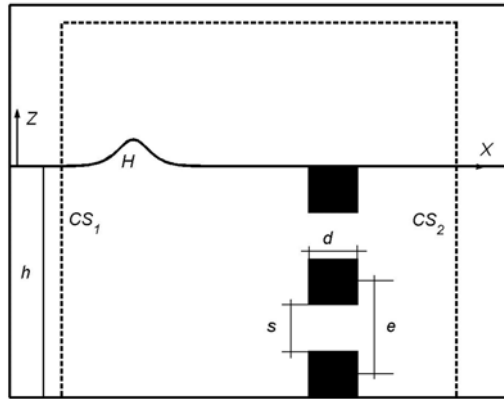


Figure 1. Numerical set-up (the sketch is not to scale)

Wave Reflection

From the tabulated results in table 1, it is clearly seen that the reflection coefficient is inversely proportion to P values. From the time history of the numerical wave gauge profiles located at $x=1.0$ m (upstream) and $x=59$ m (downstream) of the breakwater as shown in figure (2a, b), it is clearly shown that there is more than one coherent reflected waves with different travelling times. The first wave results from the direct impact of the leading solitary wave on the front edge of the breakwater. The second has the form of a wave packet with the leading trough. This is due to the wave interaction with the rear edge of the breakwater as a result of flow expansion causing low pressure depression behind the breakwater. It is clearly shown in table 1 that even when the breakwater becomes non-porous, the amount of energy reflected can be as high as $1/2$ of the energy contained in the incident solitary wave.

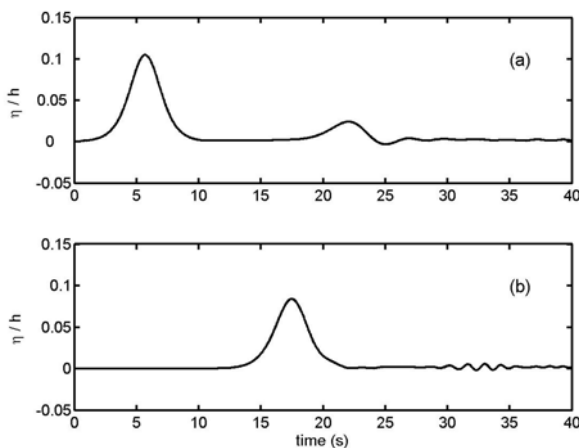


Figure 2. Time history of wave profile at $x=1.0m$ (a) & $x=59m$ (b) for $P=0.20$

In general, the calculated coefficients were quite close in all three methods due to small H/h values. The difference was less than 5.0%. It seems that the calculated coefficients from linear wave

theory give reasonable upper-bound estimations for small H/h values.

Wave transmission

The transmission coefficients in all tests were above 0.50 and highly dependent on porosity P values of the breakwater. It is seen that the transmission coefficient decreases when P gets smaller until it reaches approximately ~ 0.60 when the breakwater behaves as a non-porous structure. When the porosity P is small, the solitary wave undergoes a fission process. The fission process will generate a packet of small trail surface waves after passing through the breakwater. The trailing surface waves travel at a speed much slower than the main soliton which preserves the soliton shape. The amplitude of the small surface waves decays fast with time (see Figure 2b). The transmission coefficient is quite close in all three methods except when $P=0.10$ and 0.20 . From method 3 results, a consistent over-prediction of the coefficient is observed.

Energy dissipation

Wave energy dissipation has an important role during solitary wave interaction with the porous breakwater. Thus the main portion of energy losses comes from vortex generation as the flow travelling through the porous in the breakwater causes pressure differences across the breakwater. Consequently, the fluid particles experience deceleration as it travels through the porous away from the breakwater. These features are usually observed in shear flow and cause flow separation. Vortex shedding is very significant in this study and considered to be the main mechanism for energy dissipation. The energy dissipation works against wave transmission and the amount of energy loss can be as high as ~ 0.70 of the energy contained in the incident wave. The maximum value for the energy dissipation coefficient occurs when the breakwater becomes almost non-porous structure (obstacle). This is totally due to flow separation and enhanced vortex generation at the corner of the breakwater edges. The turbulence associated with vortical flows can be very significant. These observations were reported and can be found in numerous literature. In all cases, the energy dissipation coefficient is larger than the wave reflection coefficient.

Table 1: K_r , K_t , and K_d coefficients for different P values

P	K_r			K_t			K_d		
	M.1	M.2	M.3	M.1	M.2	M.3	M.1	M.2	M.3
0.00	0.45	0.48	0.46	0.58	0.58	0.60	0.68	0.66	0.66
0.10	0.29	0.34	0.33	0.64	0.70	0.69	0.71	0.63	0.64
0.20	0.18	0.22	0.21	0.79	0.82	0.83	0.59	0.53	0.52
0.50	0.03	0.04	0.04	0.97	0.98	0.98	0.24	0.20	0.20

CONCLUDING REMARKS

The hydraulic performance of submerged porous breakwater under solitary wave attack is investigated numerically with a well validated RANS model for different porosity P values. For the sets of numerical experiments only the weakly nonlinear solitary waves ($H/h = 0.1$) were considered. Three different methods were used to calculate the energy coefficients. Method 1 considered the integral energy equation for turbulent flows as the basis for the calculation of wave energy coefficients. In this method, the pressure induced energy flux and convective energy flux were retained to ensure the wave nonlinearity is considered. In general,

method 1 gives less reflection and transmission coefficient values than any other methods (2 & 3) and higher dissipation coefficient. In method 2, the equal partition assumption was asserted in the study to predict the total energy based on the calculation of the potential energy of the free surface displacement at different locations along the domain. The equal partition approach can predict the total energy very well especially when the waves are weakly nonlinear. In general, method 2 slightly over-estimates the transmission especially when $P=0.10$ coefficient. In method 3, the assumption of the linear wave theory was applied. It is obvious that this method would give over-estimated values for transmission coefficients and under-estimate the dissipation coefficient.

In the present study, the submerged porous breakwater kept the reflected and transmitted coefficients below 0.50 and above 0.60 respectively. Thus, the submerged porous breakwater would be an excellent option for coastal soft defence structures that are able to enhance water circulation and exchange between open sea and sheltered areas. The minimum energy dissipation of the submerged porous breakwater observed, when the porosity was $P=0.50$, is roughly $\sim 1/4$ of the total energy. The energy dissipation would contribute significantly to the reduction of the transmission coefficient. In conclusion, although method 2 & 3 can reasonably predict the reflection and transmission coefficients very well, the energy dissipation coefficient is always underestimated. Intuitively, the discrepancies between methods do exist since both methods (2 & 3) do not consider the nature of the flow which exhibit flow separation, vortex generation and turbulence. To rigorously test and validate method 1, a set of numerical experiments for highly nonlinear waves are required to ensure the convective energy flux becomes important in the integral energy equation for general turbulent flows. This requirement is important to compare the hydraulic performance of submerged porous breakwaters (energy coefficients) with any other methods. Some results will be presented to shed some insight regarding the claim discussed above involving choosing highly nonlinear waves ($H/h = 0.3$) with a similar numerical set up. We note that the results are preliminary and have not been thoroughly investigated. When porosity ($P = 0.50$) and $H/h = 0.30$, the discrepancies due to wave nonlinearity can be clearly noted in calculating the energy coefficients by the three methods. The result summarises that energy dissipation coefficients are $K_d = 0.39, 0.28$ and 0.29 for method 1, 2 and 3 respectively. However, we believe to gain a better and complete understanding of the performance of the submerged porous breakwater, we should test the effectiveness of wave nonlinearity on the calculated energy coefficients. Therefore, the effect of highly nonlinear solitary waves $H/h > 0.10$ and breakwater width d on the hydraulic performance of submerged porous breakwater will be reported elsewhere.

REFERENCES

- AL-BANAA, K. A. (2005). An experimental and numerical investigation of the interaction of non-breaking long-waves with a 2-D surface piercing-type rigid thin vertical barrier, Ph.D. dissertation, Cornell University, USA.
- CHANG, K.-A., HSU, T.-J. and LIU, P.L.-F (2001). Vortex generation and evolution in water waves propagating over a submerged rectangular obstacle: Part I. Solitary waves, *Coast Eng.* 44, 13-26.
- CHANG, K.-A., HSU, T.-J. and LIU, P.L.-F (2005). Vortex generation and evolution in water waves propagating over a submerged rectangular obstacle: Part II. Cnoidal waves, *Coast Eng.* 52, 257-283.
- GORING, D. G. (1979). Tsunamis- The propagation of long waves onto a shelf. Cal. Inst. Tech., CA. Rep. No. KH-R-38.
- GRILLI, S. T., LOSADA, M. A. and MARTIN, F. (1994). Characteristics of solitary wave breaking induced by breakwaters. *J. Waterw. Port Coast. Ocean Eng.* 118 (1), 74-92.
- HIRT, C. W., and NICHOLS, B. D. (1981). Volume of fluid (VOF) method for the dynamics of free boundaries, *J. Of Comp. Phys.*, 39, 201-225.
- LEE, J. -J., SKJELBREIA, J. E., RAICHLIN, F. (1982). Measurement of velocities in solitary waves, *J. Waterw. Port Coast. Ocean Eng.* 108, 200-218.
- LIN, P. and LIU, P.L.-F (1998 a). A numerical study of breaking waves in the surf zone, *J. Fluid Mech.*, 359, 239-264.
- LIN, P. and LIU, P.L.-F (1998 b). Turbulence transport, vorticity dynamics, and solute mixing under breaking plunging waves in surf zone. *J. Geophys. Res.* 103 (C8), 15677-15694.
- LIN, P. and LIU, P.L.-F (1998a). A numerical study of breaking waves in the surf zone, *J. Fluid Mech.*, 359, 239-264.
- LIN, P., CHANG, K.-A., and LIU, P.L.-F (1999). Run-up and rundown of solitary waves on sloping beaches, *J. Waterw. Port Coast. Ocean Eng.* 125 (5), 247-255.
- LIN, P. (2004). A numerical study of solitary waves interaction with rectangular obstacles, *Coast Eng.* 51 (1), 35-51.
- LIU, P.L.-F, LIN, P., CHANG, K.-A., and SAKIYAMA, T., (1999). Numerical modelling of wave interaction with porous structures, *J. Waterw. Port Coast. Ocean Eng.* 125 (6), 322-330.
- LIU, P.L.-F, and CHENG, Y. (2001). A numerical study of the evolution of solitary over a shelf, *Phys. Fluids* 13 (6), 1660-1667.
- LIU, P.L.-F, and AL-BANAA, K. A. (2004). Solitary wave run-up and force on a vertical barrier, Numerical modelling of wave interaction with porous structures, *J. Fluid Mech.* 505, 225-233.
- SEABRA-SANTOS, F. J., RENOUEAU, D., TEMPERVILLE, A., (1987). Numerical and experimental study of the transformation of a solitary wave over a shelf or isolated obstacle, *J. Fluid Mech.* 176, 117-134.

ACKNOWLEDGEMENTS

The author wishes to thank the Kuwait Institute for Scientific Research (KISR) for providing the financial support for this study. The author is also grateful to Prof. Philip L.-F. Liu for his support and guidance.